PANS Method as a Computational Framework from an Industrial Perspective

B. Basara

Abstract Although Computational Fluid Dynamics (CFD) is routinely used in a wide variety of industries, there are many remaining challenges in physical modelling as well as in numerical methods, which have to be tackled and eventually solved in the near future. Turbulence modelling, especially for industrial CFD, is still one of those open issues. For the purpose of a better and more practical or affordable representation of turbulence in complex flows, the variable resolution methods have emerged as an alternative to a computationally more costly Large Eddy Simulation (LES) method. At present, and among many approaches, the Partial-Averaged Navier Stokes (PANS) approach is one of the most attractive methods for industrial CFD. Therefore, the capabilities of the PANS on a wide range of CFD applications are shown in this paper. The results are presented for simple and well established benchmarks but also for industrial flows in complex geometries. The basic theory and arguments for the usage of this method are given. Besides the present status, the paper also provides some hints for possible improvements and explains some of the on-going activities in this field.

1 Introduction

Ideas about a turbulence closure method which can be used at all levels of scale resolution have been intensively pursued in the last two decades. From the beginning, such 'smart' models, which should provide the optimum solution on any computational mesh, have been very attractive to CFD users, especially to those involved in simulations of complex industrial flows. Presently, a large majority of industrial users tend to ignore the importance of turbulence models as long as calculation results are in a line with the expectations (based on the measurements or just from the experience) and simulations provide the correct behavior or relative differences in the case

B. Basara (✉)
Advanced Simulation Technology, AVL List GmbH,
Hans-List-Platz 1, 8020 Graz, Austria
e-mail: branislav.basara@avl.com

S. Girimaji et al. (eds.), *Progress in Hybrid RANS-LES Modelling*,
Notes on Numerical Fluid Mechanics and Multidisciplinary Design 130,
DOI 10.1007/978-3-319-15141-0_1

of parametric studies. The Reynolds-Averaged Navier-Stokes (RANS) turbulence models have done a good job for decades, but in many applications, the limitations of such an approach, regardless of which RANS turbulence model is used, could be a large source of the calculation error especially when the absolute accuracy is targeted. Indeed, one could recommend the best or the optimum RANS turbulence model for a certain application but there will always be some 'gray zones' in such guidelines especially for the complex industrial flows. On the other hand, the Large Eddy Simulation approach has been more frequently used in the last years but mainly for benchmarks or visibility studies. This is still due to high computational costs. One should also bear in mind that results obtained by the Large Eddy Simulation have to be carefully analyzed in order to conclude if they are trustworthy, which could be a very difficult task for everyday use in industry. And, if the conclusion is that the mesh is too coarse, the new mesh has to be created and calculations must be repeated.

Therefore, there is a clear gap between the RANS and LES simulations which require a deep knowledge in turbulence modelling, both RANS and LES, which is just one of the fields that modern simulation engineers have to cover. Therefore, the models like PANS should be the right answer for the industry. It provides the best possible physical fidelity on any given numerical grid, while varying seamlessly between Reynolds-Averaged Navier-Stokes (RANS) model and Direct Numerical Simulations (DNS). This means that the user makes calculations on the affordable mesh and the model itself combines RANS and DNS by using the arbitrary cutoff length scale concept. The PANS method belongs to the bridging (seamless) variable resolution methods which mean that the basic model is employed in the entire domain. Contrary to this group, zonal methods divide a solution domain into two modeling regions: the RANS turbulence model near the wall and the Large Eddy Simulation (LES) in the rest of the flow domain. An important drawback of zonal methods is a definition of the interface between different modeling zones, especially for complex flows.

In recent years, the bridging methods have become very popular for simulations of complex turbulent flows. Probably, the most attractive bridging method is the Partially-Averaged Navier-Stokes (PANS) formulated by Girimaji [6, 8]. This method is derived from the RANS model equations. It inevitably improves results when compared with its corresponding RANS model if more scales of motions are resolved. The PANS model is used in the industry more than other seamless methods due to its simplicity, robustness and recent theoretical extensions as well as due to the detailed validations on the number of complex cases presented in many publications. It was shown in previous studies that the implied cut-off for the PANS method can be placed in any part of the spectrum including the dissipation range. This is done by varying the unresolved-to-total ratios of kinetic energy (f_k) and dissipation (f_e). In practice, the parameter which determines the unresolved-to-total kinetic energy ratio is defined by using the grid spacing and calculated integral length scale of turbulence. If the resolution parameters, f_k and f_e, are equal unity, the PANS model recovers the RANS model. As Girimaji pointed out in his work, the better the RANS model is, the better the corresponding PANS model will be. On the other side, if the resolution parameters are very low, then the modeling of the small unresolved scales

will affect the overall solutions less. The main target of such an approach is to have an optimum turbulence model for any mesh used in calculations. There are different ways to define the resolution parameter f_k and the work presented here will show the differences between various approaches as this is a crucial point to get the PANS method widely used in the industry. We already know that numerical meshes for most industrial applications are usually coarser near the wall to achieve so-called a wall-resolved LES. A similar situation is related to PANS calculations: one could expect that f_k is equal or close to unity which means that the RANS model is used near the wall. This issue is getting more pronounced for separating flows from the curvature rather than from sharp edges. Therefore, we use the PANS variant [3] derived from the four equation near-wall eddy viscosity transport model, namely k-ε-ζ-f turbulence model [11]. As this model represents a practical and accurate RANS choice for a wide range of industrial applications, especially when used in conjunction with the universal wall approach, its PANS variant therefore guarantees that the proper near-wall model is used when f_k is of a higher value. The paper presents a variety of test cases, from simple flow benchmarks to complex industrial flows. The results will show that this modeling approach can be successfully used for complex industrial applications.

2 Computational Method

The partially-Averaged Navier-Stokes equations are written in term of partially averaged or filtered velocity and pressure field, thus

$$\frac{\partial U_i}{\partial t} + U_j \frac{\partial U_i}{\partial x_j} + \frac{\partial \tau\left(V_i, V_j\right)}{\partial x_j} = -\frac{1}{\rho}\frac{\partial p}{\partial x_i} + \nu \frac{\partial^2 U_i}{\partial x_j \partial x_j} \tag{1}$$

where the velocity field is decomposed into two components, the partially filtered component and the sub-filter component as

$$V_i = U_i + u_i \tag{2}$$

The closure for the sub-filter stress can be obtained by using the Boussinesq approximation as

$$\tau\left(V_i, V_j\right) = -2\nu_u S_{ij} + \frac{2}{3} k_u \delta_{ij} \tag{3}$$

where the eddy viscosity of unresolved scales and the resolved stress tensor are equal to

$$\nu_u = c_\mu \frac{k_u^2}{\varepsilon_u} \qquad S_{ij} = \frac{1}{2}\left(\frac{\partial U_i}{\partial x_j} + \frac{\partial U_j}{\partial x_i}\right) \tag{4}$$

and the resolution parameters are

$$f_k = \frac{k_u}{k} \qquad f_\varepsilon = \frac{\varepsilon_u}{\varepsilon} \tag{5}$$

However, values of these parameters can be checked only at the end of calculations but they are needed at the start of calculations and even at the start of every time step. This input unresolved-to-total kinetic energy ratio f_k is therefore based on the grid spacing [3, 7], thus

$$f_k \geq \frac{1}{\sqrt{c_\mu}} \left(\frac{\Delta}{\Lambda} \right)^{2/3} \tag{6}$$

where Δ is the grid cells dimension and $\Lambda = (k^{3/2}/\varepsilon)$ is the integral scale of turbulence, while f_ε was taken to be equal 1. A dynamic parameter f_k changes at each point at the end of every time step, and then it is used as a fixed value at the same location during the next time step. Note that at the end of calculations or at the end of each time step, it must be ensured that

$$\frac{1}{\sqrt{c_\mu}} \left(\frac{\Delta}{\Lambda} \right)^{2/3} \geq \frac{k_u}{k} \tag{7}$$

In other words, the parameter f_k, which is imposed on calculations, should be at the end supported by the mesh. It is also important to know that the PANS method produces the correct production-to-dissipation ratio which changes gradually from RANS value to DNS value as f_k, is reduced from 1 to 0. This is analytically proven in the paper of Girimaji [8]. This is clear evidence that PANS captures all intermediate resolution with precision. The original model of Girimaji [8], which provides the unresolved kinetic energy equations

$$\frac{Dk_u}{Dt} = P_u - \varepsilon_u + \frac{\partial}{\partial x_j} \left[\left(\nu + \frac{\nu_u}{\sigma_{ku}} \right) \frac{\partial k_u}{\partial x_j} \right] \tag{8}$$

and the unresolved energy equation

$$\frac{D\varepsilon_u}{Dt} = C_{\varepsilon 1} P_u \frac{\varepsilon_u}{k_u} - C^*_{\varepsilon 2} \frac{\varepsilon_u^2}{k_u} + \frac{\partial}{\partial x_j} \left[\left(\nu + \frac{\nu_u}{\sigma_{\varepsilon u}} \right) \frac{\partial \varepsilon_u}{\partial x_j} \right] \tag{9}$$

with the new constants, thus

$$C^*_{\varepsilon 2} = C_{\varepsilon 1} + \frac{f_k}{f_\varepsilon} \left(C_{\varepsilon 2} - C_{\varepsilon 1} \right); \sigma_{ku,\varepsilon u} = \sigma_{k,\varepsilon} \frac{f_k^2}{f_\varepsilon} \tag{10}$$

is extended by Basara et al. [3] for more accurate near-wall modelling. This new PANS variant, namely PANS k-ε-ζ-f, solves additional equations, thus

$$\frac{D\zeta_u}{Dt} = f_u - \frac{\zeta_u}{k_u}P_u + \frac{\zeta_u}{k_u}\varepsilon_u\left(1 - f_k\right) + \frac{\partial}{\partial x_j}\left[\left(\nu + \frac{\nu_u}{\sigma_{\zeta_u}}\right)\frac{\partial \zeta_u}{\partial x_j}\right] \tag{11}$$

$$L_u^2\nabla^2 f_u - f_u = \frac{1}{T_u}\left(c_1 + C_2'\frac{P}{\varepsilon}\right)\left(\zeta_u - \frac{2}{3}\right) \tag{12}$$

with the unresolved eddy viscosity now taken as

$$\nu_u = C_\mu \zeta_u \frac{k_u^2}{\varepsilon_u} \tag{13}$$

Constants c_1 and C_2' are taken as proposed in the original model. L_u and T_u are the length and time scales defined by using unresolved kinetic energy respectively. It is clear that for $f_k = 1$, the equation for ζ_u will get its RANS form. Note also that $f_\varepsilon = 1$ implies that $\varepsilon_u = \varepsilon$.

The approach shown above has been proved on large number of cases which include static meshes. The main issue is that the total kinetic energy needed for the integral length scale and for the input of f_k can be accurately calculated only after averaged field is obtained, thus

$$k = k_r + k_u \tag{14}$$

where the resolved turbulence is obtained from

$$k_r = \frac{1}{2}\left(U_i - \overline{U_i}\right)^2 \tag{15}$$

This means that for the calculation of the resolved part, we need the average velocity which is impractical for the moving meshes (e.g. engines) or cases with transient boundaries.

Nevertheless, it was shown in the past that for the static mesh cases, the PANS method presented above can produce practical, accurate and reliable results. In order to avoid averaging the velocity field and calculation the resolved kinetic energy, Basara and Girimaji [9] derived the additional equation for so called the scale supplying variable which actually represents the modelled resolved kinetic energy. This equation is derived by using the PANS basic principles and following the similar procedure as done for the unresolved kinetic energy shown above. The equation can be written as

$$\frac{Dk_{ssv}}{Dt} = \frac{k_{ssv}}{k_u}\left(P_u - \varepsilon_u\right) + \frac{\partial}{\partial x_j}\left[\left(\nu + \frac{\nu_u}{\sigma_{ku}}\right)\frac{\partial k_{ssv}}{\partial x_j}\right] \tag{16}$$

Note that the total kinetic energy is now calculated as

$$k = k_{ssv} + k_u \tag{17}$$

The results are shown in the next section.

There are other possibilities to predict f_k. Recently Foroutan and Yavuzkurt [5] proposed the formulation for f_k which ensures that the predicted value is between 0 and 1, thus

$$f_k = 1 - \left[\frac{\left(\frac{\Lambda}{\Delta}\right)^{2/3}}{0.23 + \left(\frac{\Lambda}{\Delta}\right)^{2/3}} \right]^{4.5} \tag{18}$$

Values of f_k predicted with Eq. (18) are lower in general than those obtained with Eq. (6). In any case it must be checked that Eq. (7) is satisfied especially in the near wall region.

It is also worth of revisiting the work of Speziale [15], see also Hussaini et al. [10], who provided a possible path in deriving the f_k value in the form of

$$f_k = \left[1 - \exp\left(-\beta \Delta / \Lambda_k\right)\right]^n \tag{19}$$

where β and n are constants.

This modelling approach is further enhanced by including the hybrid wall treatment. This entails combining integration up to the wall with wall functions. Smoothing functions which blend two formulations together are known by different names: automatic, hybrid or compound wall treatments (see [2, 14]). The blending formula for the quantities specified at the cell next to the wall is given as

$$\phi = \phi_\nu e^{-\Gamma} + \phi_t e^{-1/\Gamma} \tag{20}$$

where 'ν' is the viscous and 't' the fully turbulent value of the variables: wall shear stress, production and dissipation of the turbulent kinetic energy. The function Γ is given as

$$\Gamma = \frac{0.01\left(y^+\right)^4}{1 + 5y^+} \tag{21}$$

This ensures that the optimum RANS approach is used for $f_k = 1$ and any distance from the wall (any y^+ values).

The concept presented in this section implies that there are regions with spatial or temporal variations in filter width. Hence, Wallin and Girimaji [16] and Wallin et al. [17], have introduced commutation residual terms in the resolved momentum and unresolved kinetic energy equations in the context of the PANS approach (see also [9]). It is easy to implement proposed modifications in the computer code and there are no additional penalties in calculations, see original references.

This brief review shows the present status and the focus of on-going activities related to the PANS method.

2.1 Numerical Method

The PANS model is implemented into the commercial CFD code AVL FIRE. All dependent variables, such as momentum, pressure, density, turbulence kinetic energy, dissipation rate, and passive scalar are evaluated at the cell center. The cell-face based connectivity and interpolation practices for gradients and cell-face values are introduced to accommodate an arbitrary number of cell faces. A second-order midpoint rule is used for integral approximation and a second order linear approximation for any value at the cell-face. The convection is solved by a variety of differencing schemes (upwind, central differencing, MINMOD, and SMART). The rate of change is discretized by using implicit schemes, namely Euler implicit scheme and three time level implicit scheme of second order accuracy. The overall solution procedure is iterative and is based on the Semi-Implicit Method for Pressure-Linked Equations algorithm (SIMPLE). For the solution of a linear system of equations, a conjugate gradient type of solver and algebraic multi-grid are used.

3 Results and Discussion

The predictive performances of the PANS k-ε-ζ-f model are shown on few examples below. Note also that these results are extracted here from various systematic studies just to emphasize certain important points in calculations specific to the PANS usage.

3.1 Channel Flow

PANS calculations for the channel flow with the $Re_\tau = 650$ based on the wall friction velocity u_τ, the channel half width δ and kinematic viscosity ν is analyzed in the work of Basara et al. [3] in all detail. Direct Numerical Simulation data of Iwamoto et al. [12] was used for comparisons. Instantaneous iso-surfaces of the second invariant of the velocity gradient as computed by PANS on two meshes are shown in Fig. 1 (left), (right). Following Eq. (6) the ratio between unresolved-to-total kinetic energy f_k will be decreased with the grid refinement and consequently finer structures are captured. The present standard procedure with the PANS method is to use Eq. (6) for f_k which provides typical variable instantaneous values as shown in Fig. 2 (left). However, using the most recent development described by Eqs. (16, 17), predicted f_k will vary less than with the standard approach as shown in Fig. 2 (right). However, the averaged velocity is close to each other and a very good agreement with DNS data is obtained, see Fig. 3 (left).

It is useful to know that fluctuating f_k helps clearly to capture instantaneous flow and the smooth f_k could lead to the steady flow without predicting any small structures. But even 'smooth' f_k values if they are low, as shown in Fig. 2 (right) will lead to the fluctuating velocities. Note also that the condition given by Eq. (7) must be satisfied. This new method is only introduced here in order to give the answer at the

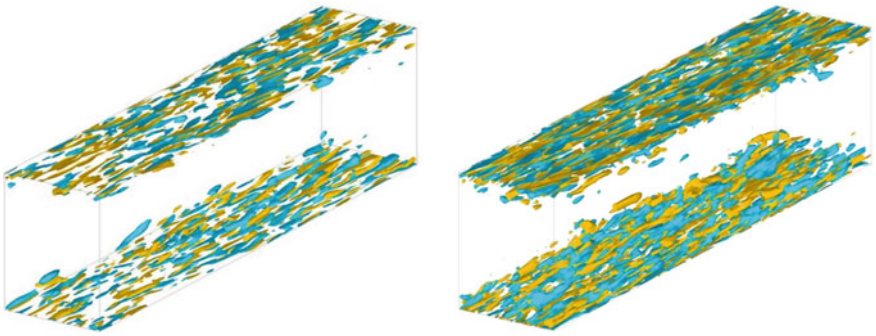

Fig. 1 An instantaneous isosurface of the second invariant of the velocity gradient as predicted by the PANS k-ε-ζ-f on different grids

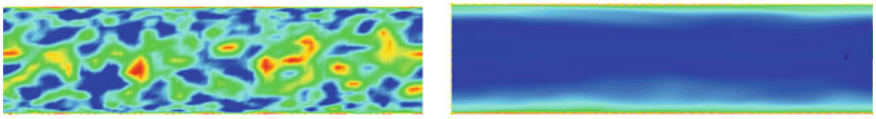

Fig. 2 Unresolved-to-total kinetic energy computed by Eqs. (6) and (14–15) (*left*) and by Eqs. (16–17) (*right*)

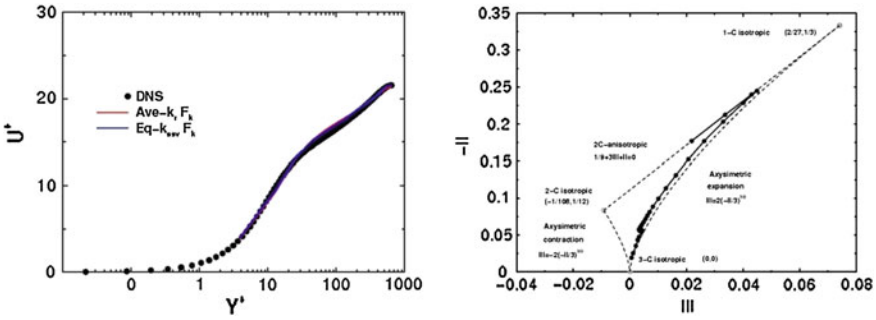

Fig. 3 Channel flow: computed mean velocity (*left*) and the predicted invariant map (*right*)

first place what can be done for the moving geometries or calculations which have transient boundaries. Otherwise, one has to apply cycle to cycle averaging which is not practical for general applications. Or, one has to start with the constant f_k and then values should be corrected for the next cycle depending of the maximum values obtained in the present cycle. This is possible to make but it would not lead to the optimum use of computer resources. However, it is important to say, that the standard method explained above is proved on many simple and complex applications.

In order to close the channel flow performance assessment, invariants of Reynolds stress anisotropy on the so-called Lumley invariant map, as predicted by the standard approach, is shown in Fig. 3 (right).

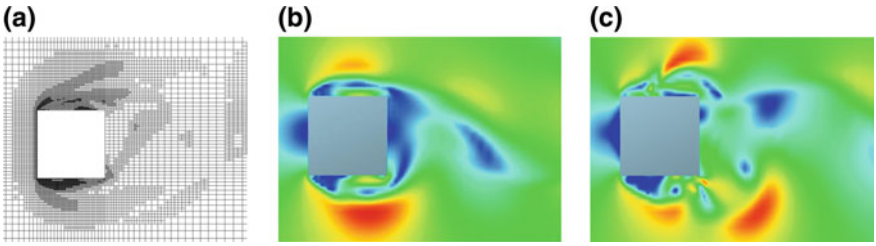

Fig. 4 Mesh sequence after the adaptive grid refinement (**a**), the predicted velocity magnitude on the coarse mesh (**b**) and on the fine mesh (**c**)

The behavior of the invariants in the wall-normal direction provides the strongest indication of the fidelity of the model calculation.

3.2 Square Cylinder

Data for the vortex shedding flow around a square cylinder at Re = 21,400 is available in the ERCOFTAC classic database. The PANS predictions are well described in the work of Basara and Pavlovic (2010). A direct effect of the automatic mesh refinement is shown here as well. Cells, which have f_k values larger than 0.5, are refined. Only two refinements starting on the mesh containing 30,000 cells are applied. Meshes created with the refinement have the size 408,000 and 696,700 cells. The extract of the finest mesh is shown in Fig. 4a, and the velocity magnitude on the second mesh is shown in Fig. 4b and on the finest mesh in Fig. 4c. It is easy to observe that smaller structures are captured with the mesh refinement.

Predicted time-averaged velocity and time-averaged turbulent kinetic energy are shown in Fig. 5 (left), (right). Results are very much improved with the mesh refinement. It is the same effect as by using meshes refined in advance, but with the adaptive

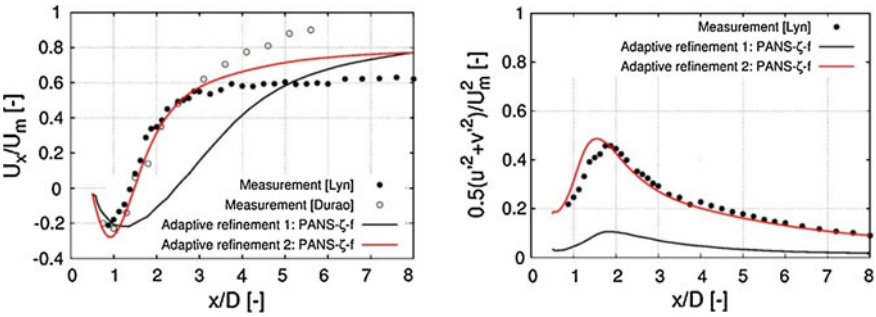

Fig. 5 Time-averaged velocity (*left*) and turbulent kinetic energy (*right*) along the *centre line* and behind the *square cylinder* computed on meshes which are refined based on f_k

meshes, the whole approach is even more practical especially for the industrial CFD users.

3.3 External Car Aerodynamics

There are number of publications dealing with the performance of RANS turbulence models for the external car aerodynamics. In general, the agreement with measurements for the drag coefficient is in the range of $(+/-)$ 3 %. There are exceptional cases where the unsteady effects dominate and the error goes up to 10 %. The recent paper of Jakirlic et al. [13] presents improvements achieved with the PANS in comparisons with RANS and Unsteady RANS (URANS) approaches. It is generally accepted that the prediction of the lift coefficient brings more uncertainties when the RANS models are used. For the car aerodynamics test case, the simplified Volvo VRAK 1:1 experimental model is used. The complete description of the geometry is given in Krajnovic et al. [3]. The inlet velocity is given as 38.9 m/s. The numerical grid has 4.5 million computational cells. Even on so coarse mesh, the PANS model could predict small structures which cannot be captured with the RANS models, see Fig. 6. Predicted lift coefficient is shown in Table 1. A very good agreement with the measured data is achieved. Although the same numerical mesh was used, large improvements in the predicted lift coefficient have been observed.

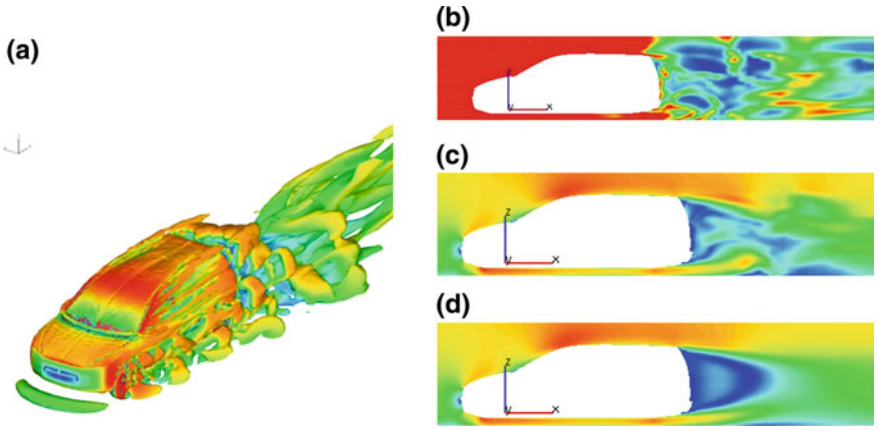

Fig. 6 Predicted flow structures around the car (**a**), f_k (**b**), instantaneous (**c**) and averaged velocities (**d**)

Table 1 Measured and calculated lift coefficient

Data	0.026
RANS k-ε-ζ-f	0.054
PANS k-ε-ζ-f	0.030

Figure 6b shows the resolution parameter f_k which varies from 0 (blue) to 1 (red). This is a typical distribution of f_k, the larger part of a domain in front and above the car is covered by the RANS model and in the wake with the full variable resolution PANS model (note that for $f_k = 1$ the PANS recovers into the RANS approach). Figure 6c shows the averaged velocity as predicted with the PANS. Calculation time needed for PANS is similar to LES calculations; the CPU needed for additional equations is small compared to time needed to average results.

3.4 Intake Port

Typical intake port configuration is shown in Fig. 7. The mesh consisted of 4 million cells have been used. The constant total pressure is specified at the inlet and the static pressure is specified at the outlet. The following parameters in the cylinder were compared:

(a) Torque: $M_t = \sum \rho_i (\vec{U}_i \times \vec{r}_i) \cdot \vec{n} \cdot U_{ax} \cdot A_i$ (r_i is the radius, $\vec{n}$ is the normal vector, U_{ax} axial velocity and A_i stands for the area)
(b) Swirl number: $SN = \frac{n_{Mt}}{n_{Eng}}$ (n_{Mt} is a torque speed and n_{Eng} is an engine speed).

Figure 7 (right) shows an instantaneous parameter f_k which determines the unresolved-to-total kinetic energy ratio which is in the range between 0 and 1. In the region where f_k is equal 1, the RANS k-ε-ζ-f model is used. Following this parameter, it can be seen where the mesh should be refined to further improve results.

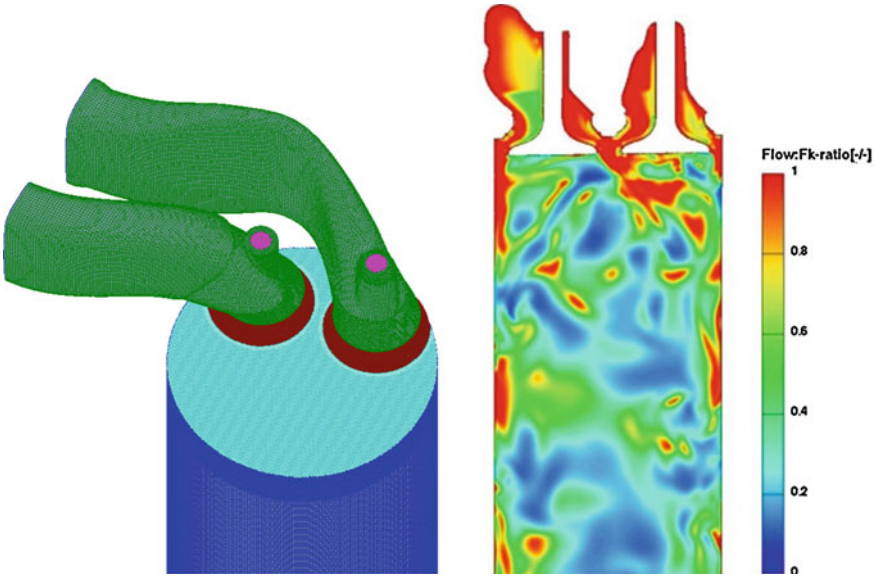

Fig. 7 The mesh for the intake port (*left*) and the predicted instantaneous resolution parameter f_k (*right*)

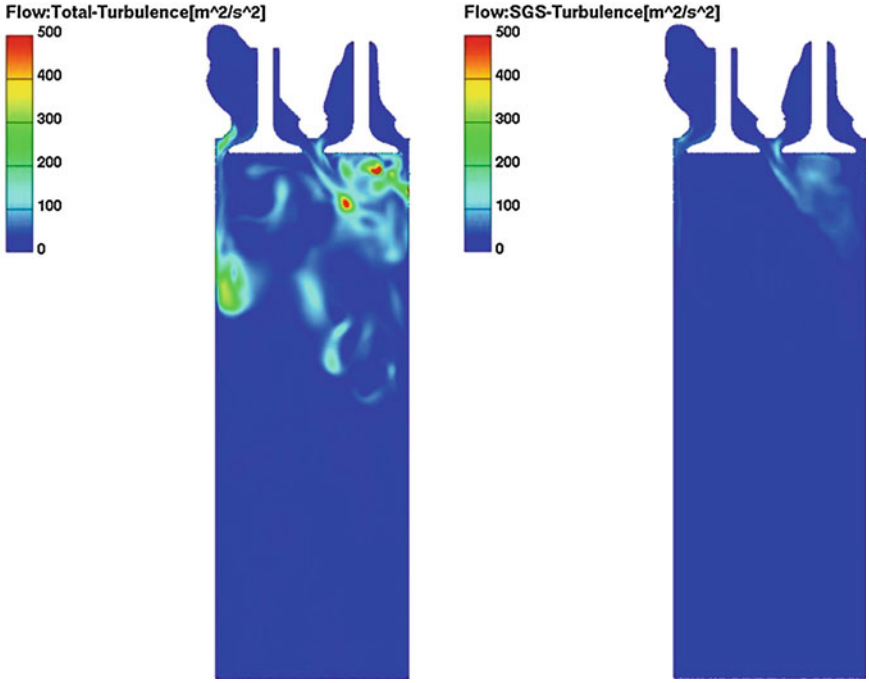

Fig. 8 Predicted total (*left*) and unresolved (*right*) turbulent kinetic energy

Note also that in the near wall region, a dynamic parameter which determines the unresolved-to-total kinetic energy ratio f_k is equal 1, and hence there, an appropriate near wall RANS model should be used.

Figure 8 shows the total and the unresolved kinetic energy as predicted by the PANS model. This should be always monitored. The unresolved (or SGS) kinetic energy will decrease with the mesh refinement, and the model used for the modeling of the unresolved kinetic energy becomes less important.

Predicted torque was 0.0161 and 0.014 with the RANS and PANS models respectively. The PANS k-ε-ζ-f provided the value closer to the measured value of 0.012. The same is with the swirl number where the PANS model reached 1.90 which is closer to the measured value of 1.65 when compared to the RANS results of 2.31.

3.5 Engine

The next case is the engine case with meshes suitable for RANS rather than for LES calculations (just used for the purpose of explaining the new approach for obtaining the value for f_k). In average, there are 1–1.5 million cells used per time step. Figure 9 shows the mesh just for the illustration of the computational domain and the turbulent

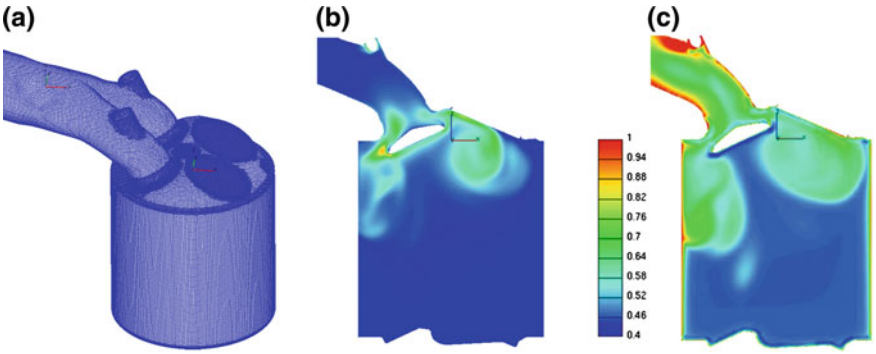

Fig. 9 Engine case: the standard mesh for RANS calculations (**a**), a turbulent kinetic energyas predicted by RANS (**b**) and the resolution parameter predicted by using Eq. (6) (**c**)

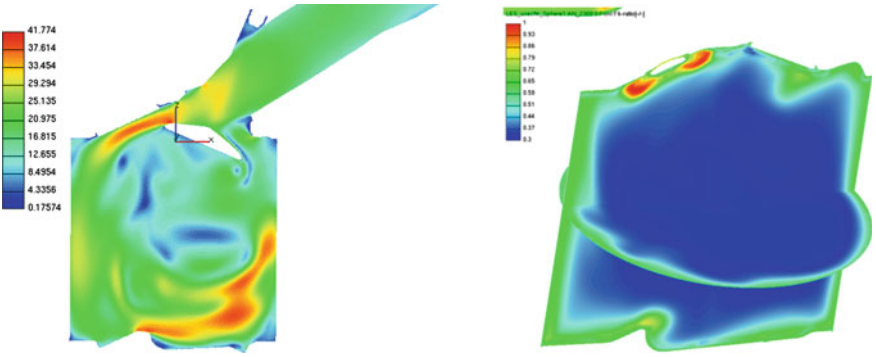

Fig. 10 Predicted instantaneous velocity magnitude (*left*) and the resolution parameter f_k (*right*)

kinetic energy as calculated by the RANS k-ε-ζ-f model (see Fig. 9a, b). This kinetic energy is the total energy represented by the RANS and it is used to estimate the suitability of this mesh for the LES or the hybrid RANS/LES calculations. Figure 9c shows the result of Eq. (6) with the predicted minimum value of 0.4 in the cylinder. It could be said that this is not an appropriate mesh for LES calculations but we have done it just for the purpose of the comparisons with PANS calculations.

In order to avoid averaging the velocity field and calculating the resolved kinetic energy, the formulation of Basara and Girimaji [4] given by Eqs. (16, 17) is used here. Now, this procedure is applied on the full engine case. Figure 10 (right) shows the instantaneous f_k which is different than one based on the RANS calculations shown in Fig. 9c, but overall has similarities. This is of course due to different turbulence level predicted by two approaches; see also the instantaneous velocity predicted by the PANS as shown in Fig. 10 (left). It should be also reported that for this particular mesh, cycle to cycle variations obtained by LES are double larger than obtained with PANS calculations (20 vs. 10 % which is closer to the measured value of 30 %).

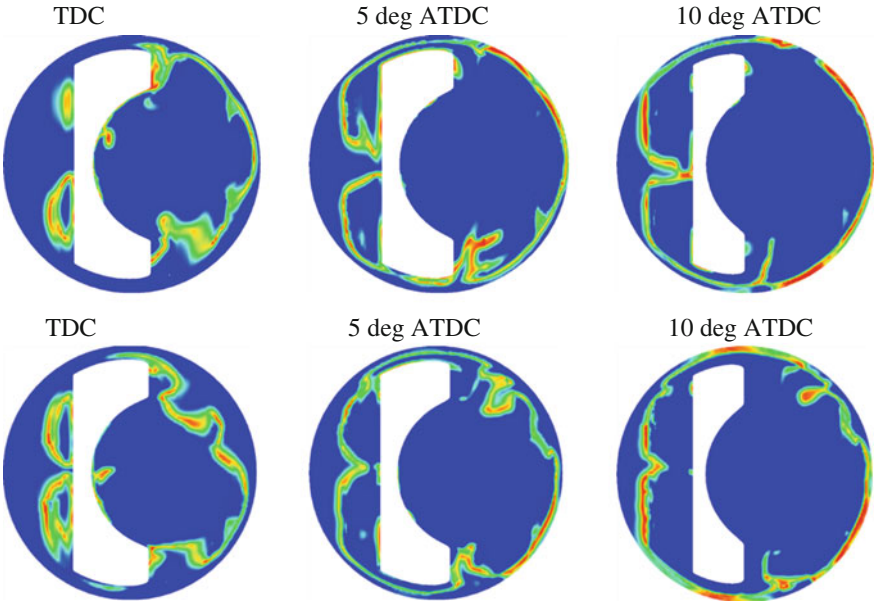

Fig. 11 The flame front position at different time steps as predicted with the PANS model

However, one could expect that these are spurious oscillations caused by inaccuracy of LES on the coarse mesh.

The flame front position as predicted with the PANS is shown in Fig. 11 for three different time steps in two neighbouring cycles. It is visible that the flame front position is different. Note that the combustion modelling was done the same way as for LES, the unresolved kinetic energy obtained by Eq. (8) just replaces the sub-grid scale kinetic energy provided by LES. The rest of modelling is the same.

4 Conclusions

The basis of the PANS method is briefly outlined and some representative results are shown. It should be pointed out that the code which employs the PANS model, in this case k-ε-ζ-f variant, can easily switch from the steady state RANS ($f_k = 1$ and no transient terms), to unsteady RANS ($f_k = 1$ and including transient terms) and to the variable resolution model, the full PANS approach ($f_k \neq 1$). Another advantage of this approach is that all calculations performed up to now have provided better results than those obtained by the RANS model as soon as the finer meshes are employed. The paper also shows the novel approach for calculations on moving meshes. Different variants of the PANS models as well as formulations of the resolution parameters will be tested and further improved.

Acknowledgments It is the author's pleasure to thank Dr. M. Bogensperger for setting up the engine test case.

References

1. AVL FIRE Manual, AVL List GmbH, Graz, Austria. CFD Solver Version 2013
2. Basara, B.: An eddy viscosity transport model based on elliptic relaxation approach. AIAA J. **44**(7), 1686–1690 (2006)
3. Basara, B., Krajnovic, S., Girimaji, S., Pavlovic, Z.: Near-wall formulation of the partially averaged Navier-Stokes turbulence model. AIAA J. **49**(12), 2627–2636 (2011)
4. Basara, B., Girimaji, S.: Modelling of the cut-off scale supplying variable in bridging methods for turbulence flow simulation. In: Proceedings of International Conference on Jets, Wakes, and Separated Flows, Nagoya, Japan, 17–21 Sept 2013
5. Foroutan, H., Yavuzkurt, S.: Partially-averaged Navier-Stokes modeling of turbulent swirling flow. In: American Physical Society, 66th Annual Meeting of the Division of Fluid Dynamics, Pittsburgh, Pennsylvania, 24–26 Nov 2013
6. Girimaji, S., Srinivasan, R., Jeong, E.: PANS turbulence models for seamless transition between RANS and LES; fixed point analysis and preliminary results. ASME Paper FEDSM45336, (2003)
7. Girimaji, S., Abdul-Hamid, K.S.: Partially-averaged Navier-Stokes model for turbulence: implementation and validation, AIAA Paper 2005–0502. Reno, NV (2005)
8. Girimaji, S.S.: Partially-averaged Navier-Stokes model for turbulence: a reynolds-averaged Navier-Stokes to direct numerical simulation bridging method. J. Appl. Mech. **73**, 413–421 (2006)
9. Girimaji, S.S., Wallin, S.: Closure modeling in bridging regions of variable-resolution (VR) turbulence computations. J. Turbul. **14**(1), 72–98 (2013)
10. Hussaini, M.Y., Thangam, S., Woodruff, S.L., Zhou, Y.: Development of a continuous model for simulation of turbulent flows. J. Appl. Mech. **73**, 441–448 (2006)
11. Hanjalic, K., Popovac, M., Hadziabdic, M.: A robust near-wall elliptic-relaxation eddy-viscosity turbulence model for CFD. Int. J. Heat Fluid Flow **25**(6), 1047–1051 (2004)
12. Iwamoto, K., Suzuki, Y., Kasagi, N.: Reynolds number effect on wall turbulence: toward effective feedback control. Int. J. Heat Fluid Flow **23**(5), 678–689 (2002)
13. Jakirlic, S., Kutej, L., Basara, B., Tropea, C.: Computational study of the aerodynamics of a realistic car model by means of RANS and hybrid RANS/LES approaches. SAE Int. J. Passeng. Cars Mech. Syst. **7**(2), (2014). doi:10.4271/2014-01-0594
14. Popovac, M., Hanjalic, K.: Compound wall treatment for RANS computation of complex turbulent flows and heat transfer. Flow Turbul. Combust. **78**, 177–202 (2007)
15. Speziale, C.G.: A combined large-eddy simulation and time-dependent RANS capability for high-speed compressible flows. J. Sci. Comput. **713**(3), 441–448 (1998)
16. Wallin, S., Girimaji, S.S.: Commutation error mitigation in variable-resolution PANS closure: proof of concept in decaying isotropic turbulence. In: 6th AIAA Theoretical Fluid Mechanics Conference, AIAA Paper 2011–3105. Honolulu, Hawaii, 27–30 June 2011
17. Wallin, S., Reyes, D.A., Girimaji, S.S.: Bridging between coarse and fine resolution in variable resolution turbulence computations. In: Proceeding of Turbulence, Heat and Mass Transfer, vol. 7, Palermo, Italy (2012)